NASA Technical Memorandum 83614

Heat Transfer in Serpentine Passages With Turbulence Promoters

Robert J. Boyle
Lewis Research Center
Cleveland, Ohio

Prepared for the
Twenty-second National Heat Transfer Conference
cosponsored by the ASME and AIChE
Niagara Falls, New York, August 5–8, 1984

NASA

HEAT TRANSFER IN SERPENTINE PASSAGES WITH TURBULENCE PROMOTERS

Robert J. Boyle
National Aeronautics and Space Administration
Lewis Research Center
Cleveland, Ohio 44135

ABSTRACT

Local heat transfer rates and overall pressure losses were determined for serpentine passages of square cross section. The flow entered an inlet leg, turned 180° and then passed through an outlet leg. Two series of tests were done. First, results were obtained for a passage with smooth walls for three different bend geometries. Second, the effect of turbulence promoters was investigated. Tests were done for turbulence promoters between 0.6 and 15 percent of the passage height. Gaseous nitrogen was the working fluid, and the Reynolds number varied between 20 000 and 100 000. Local heat transfer rates were determined from thermocouple measurements on a thin electrically heated Inconel foil. Pressure drop measurements were made along the flow path.

NOMENCLATURE

A_f	area of foil, m^2
C	coefficient in Eq. (4)
D	hydraulic diameter, m
e	height of turbulence promoter, m
e^+	normalized turbulence promoter height
f	friction factor
h	heat transfer coefficient $W/m^2/°C$
H_r	heat transfer ratio
K	pressure loss coefficient
k	thermal conductivity, W/m/°C
L	distance along flow path, m
Nu	Nusselt number
P	pressure, N/m^2
Pr	Prandtl number
p	pitch, m
Q_e	heat generated in foil, W
Re	Reynolds number
St	Stanton number
T	temperature, °C
V	velocity, m/sec
ρ	density, kg/m^3

Subscripts:

fd	fully developed
g	gas
w	wall
∞	far away from entrance or bend

INTRODUCTION

The efficient design of turbine blade cooling passages requires accurate heat transfer and pressure loss coefficients. Excessive coolant reduces cycle efficiency, and an error in predicting the metal temperature of 55° C can result in an order of magnitude change in blade life (Graham, 1). One approach to obtaining high internal heat transfer coefficients is to use serpentine passages with turbulence promoters on the blade walls (Holland and Thake, 2). Figure 1 shows the cooling scheme for a blade with serpentine passages with turbulence promoters on the walls. The passages are short, and have abrupt turns. The external heat transfer, and therefore, the internal cooling requirement, is not the same on the pressure and suction surfaces of the blades. Even without turbulence promoters, the flow would not be fully developed in any region of the passage. The turbulence promoters add another degree of complexity in predicting the local heat transfer. The turbulence promoters interrupt the flow adjacent to the wall, which results in higher heat transfer and pressure loss. Their use has been extensively studied, and Bergles (3) gives an extensive bibliography. However, with the exception of Burggraf's (4) data, the reported results have been for long passages, and the measurements were made in a

region where the results did not change with distance. Therefore, an experimental program was undertaken to determine heat transfer and pressure losses for short passages with turbulence promoters.

The experimental program was conducted to determine the local heat transfer within a single serpentine passage. At the inlet the flow turned 90°, passed through the inlet leg, turned 180°, and passed through the outlet leg. The test program was in two parts. In the first part smooth walls were used, and the passage geometry was varied in the bend region. In the second part turbulence promoters of different sizes were tested. The test section consisted of an inlet region, a bend region, and an outlet region.

In this report the local heat transfer rates are given as a function of the distance along the passage. Comparisons are made between the experimental heat transfer and predictions resulting from the combination of an entrance effect and fully developed heat transfer rates. From these results correlations are developed to determine the local heat transfer and pressure drop for the serpentine passages.

APPARATUS and PROCEDURE

Test Hardware

The test hardware consisted of a single serpentine passage shown in Fig. 2. Two opposite walls of the passage had electrically heated foils. For clarity only a single foil is shown in the schematic. In addition to the flow passage geometry pressure tap locations are shown. A rectangular chamber was formed using Bakelite blocks which served to insulate the test section. A Bakelite divider was used to form 1.27 cm square inlet and outlet legs of the passage. The square passage resulted in a hydraulic diameter (D) equal to the passage width. A length-to-width ratio of 15 for each leg was chosen based on the results of Boelter et al. (5). The right angle bend at the entrance was chosen because of its similarity to the bend geometry, and because it gave a long distance before flow became fully developed. The entrance to a particular blade cooling passage might be somewhat different. However, other entrances of (5) showed comparable lengths before the flow became fully developed. It is expected that the effect of the entrance on the local heat transfer in a particular blade would be similar to that for the configuration tested.

Electrically heated Inconel foils were used to simulate the blade walls. This material was chosen because its electrical resistivity did not vary with temperature, resulting in a uniform heat flux. The smooth foils were 0.05 mm thick. Figure 3 is a photograph of an instrumented foil with turbulence promoters. For most tests the turbulence promoters were an integral part of the foil, and were formed by machining an Inconel plate. These foils were approximately 0.13 mm thick between the ribs. The foils were electrically heated by a regulated dc power supply. Each foil spanned both the inlet and outlet passage, and was 2.54 cm wide. The local heat transfer coefficients were determined from individual chromel-constantan thermocouple measurements. The thermocouples were 0.13 mm in diameter, and were glued to the back of the foil along the centerline of the inlet and outlet legs. In order to achieve a good bond, they were attached over an area about 1.5 mm in diameter. Three bus bars were used. The foils could be heated individually or both together. Each copper bus bar had a thermocouple and guard heater adjacent to test sections.

The working fluid was gaseous nitrogen. A pressurized chamber was used to achieve a wide range of Reynolds numbers without having very low velocities or encountering compressibility effects. Measurements were made of flow rates, gas inlet and outlet temperatures, and pressures along the flow path.

Test Configurations

Two series of tests were run. In the first series the effect of bend region geometry on the local heat transfer was examined. All walls were smooth in this test series. Three configurations were tested, and they are shown in Fig. 4. These were a rectangular bend, a semi-circular bend, and an intermediate one with rounded corners. As can be seen in Fig. 1 the end of the blade is flat. The rectangular bend and the one with rounded corners are most representative of actual blades. The semi-circular bend was included because it does not have stagnation regions in the bend.

In the second series of tests the local heat transfer was determined for different size turbulence promoters. The height of the turbulence promoters was varied, and the passage dimensions remained the same. Rib height-to-hydraulic diameter ratios of 0.6, 5, 10, and 15 percent were tested. The rib pitch-to-height ratio was 10. The turbulence promoters had a square cross section, and were normal to the flow. All tests in this series were with a rectangular bend.

Data Acquisition

Temperatures, pressures, and voltages were digitally recorded and were continuously available on a three second update cycle. Two flow meters were used. They were a calibrated Venturi and a calibrated orifice. The electrical current was measured by the voltage drop across a calibrated shunt. The power generated in the foils was determined from resistance and current measurements.

Test Sequence

The test began by flowing gaseous nitrogen through the test section. Electrical power was applied to one or both foils. Temperatures were monitored until steady state was achieved. This took a half hour or less. Conditions were then changed by varying one of a number of parameters. These parameters included the flow rate, the heat flux, test section pressure, temperature of the bus bars, as well as the inlet gas temperature.

DATA REDUCTION

The local heat transfer rate was determined from the electrical power dissipated in the foil, the wall temperature, and the local bulk gas temperature.

$$h = \frac{Q_e/A_f}{T_w - T_g} \qquad (1)$$

The electrical power was determined from the measured foil resistance and the current in the foil. The inaccuracy in the foil resistance measurements was estimated to be less than 5 percent. This is believed to be the major uncertainty in the heat transfer measurements. Check measurements were made of the voltage drop across the foils. This gave an upper limit of the power generated in the foils, since it included

losses due to contact resistance. Measurements showed little variation in the electrical resistance per rib pitch over the length of the foils. In order to place the results on a common basis the area used was always that of a smooth foil. Since the rib pitch to height ratio (p/e) was constant, all foils with turbulence promoters had total surface areas 20 percent greater than that of a smooth foil. The wall temperature came from the thermocouple measurement. The inlet total temperature was measured in a well mixed location at the entrance to the test section. The outlet total temperature was measured in the settling chamber shown in Fig. 2. The local gas temperature was calculated assuming a linear gas temperature rise along the flow path. The reported heat transfer rates were normalized by the heat transfer rate for flow in a smooth tube with fully developed velocity and temperature profiles (McAdams, 6)

$$H_r = \frac{h\ D/k}{Nu_{fd}} = \frac{h\ D/k}{0.023Re^{.8}Pr^{.4}} \qquad (2)$$

The pressure measurements yielded loss coefficients (K), which were determined from the following equation:

$$K = \frac{\Delta P/\rho}{V^2/2} \qquad (3)$$

The density was determined from pressure and temperature measurements, and the velocity was determined from the flow rate.

RESULTS and DISCUSSION

Bend Geometry

In the initial series of tests the local heat transfer rates were determined for the three bend geometries shown in Fig. 4. For these tests all walls of the passage were smooth, and both foils were heated. Figure 5 shows the local heat transfer rate for the three bend geometries for Reynolds numbers between 20 000 and 100 000. The ordinate is the ratio of the local heat transfer rate to the rate for fully developed flow in a smooth tube (H_r). The abscissa is the distance along the centerline of the flow path. Since the flow became more fully developed as it approached the bend, the relative heat transfer rate approached 1.0 just upstream of the bend. Somewhat surprisingly, the different bend geometries did not result in significantly different heat transfer rates, even in the bend region. Each bus bar temperature was monitored, and heaters were used to increase bus bar temperatures. Variations in bus bar temperatures caused noticeable variations in the apparent heat transfer rates near the ends of the test section. This effect was accounted for by correcting the heat transfer rates to the case where the foil and bus bar temperatures were the same. The effect of bus bar temperature was most noticeable at the lowest Reynolds number, and for foil thermocouples nearest the bus bars. The data in Figs. 5(b) and (c) for Reynolds numbers of 60 000 and 100 000 show that the highest heat transfer occurred not in the bend itself, but at the start of the guided portion of the outlet leg. The data in Fig. 5(a) for a Reynolds number of 20 000 show the peak for two configurations near the end of the bend. An error in estimating the conduction to the bus bar would have the largest effect at the lowest Reynolds number. The manner in which the heat transfer changed with distance in the outlet leg was very similar to the way it changed in the inlet leg. The heat transfer rates increased with Reynolds number, but the effect of Reynolds number on the heat transfer ratio (H_r) was small. The heat transfer ratio was somewhat less at the highest Reynolds number. The local heat transfer rates did not significantly change when only one surface was heated.

The power to the foils was limited by the desire to keep the foil temperatures less than 100° C so as not to weaken the thermocouple adhesive bond. Since the accuracy was improved by maintaining the largest possible temperature difference between the gas and foils, this condition was used for most of the tests. There was no significant change in the heat transfer ratio when the power dissipated in the foils was reduced by half. This showed that any inaccuracies in the thermocouple measurements did not affect the results. The test pressure was varied by a factor of two, while the Reynolds number was held constant. This did not affect the heat transfer rates. Since the nitrogen was obtained from a high pressure source, it could enter the test section about 20° C less than ambient. Electrical tape heaters were used far upstream of the test section to control the inlet gas temperature. Most tests were run with the average gas temperature in the test section within 3° C of ambient. At this condition the amount of heat absorbed by the gas equaled the heat generated in the foils. Cold gas was useful in cool-down tests to verify thermocouple accuracy.

Pressure measurements showed the variation in pressure loss coefficient (K) was less than 0.2 for the three bend geometries tested. This value is also close to the uncertainty in the loss coefficient measurement.

Comparisons of the experimental data with a number of different predictions are shown in Fig. 6. The experimental data are for the rectangular bend at Reynolds numbers of 20 000 and 100 000. One prediction of the local heat transfer ratio is a curve from Ref. 7. This curve is the experimental data of Ref. 5 for an entrance with a right angle bend at a Reynolds number of 50 000. The four other curves were calculated using the computer code described in Ref. 8 (STAN5). Curves are given for the local heat transfer rate at Reynolds numbers of 20 000 and 100 000, for both a smooth wall and a "rough" wall. As specified in Ref. 8, the "rough" wall calculation was done by setting the damping coefficient in STAN5 equal to zero. This had the effect of having no laminar sublayer in the calculation. The experimental data and the curve from Ref. 7 show good agreement. Neither the smooth nor "rough" wall STAN5 prediction agrees with the data. The experimental data initially follow the "rough" wall prediction, but eventually agree with the smooth wall prediction. The same process occurs both at the inlet and at the start of the outlet leg. It appears that the high turbulence resulting from the abrupt change in flow direction at the start of the inlet and outlet legs results in a delay in the formation of the laminar sublayer.

Turbulence Promoter Tests

The tests with turbulence promoters were generally done with three of the four sides of the passage having smooth walls. A smooth foil was opposite the foil with turbulence promoters. Heating the smooth foil produced no change in the heat transfer rates for the foil with turbulence promoters. Figure 7 shows experimental results for 0.6 percent rib height. The data are for Reynolds numbers of 20 000 and 100 000. This small rib height was chosen because it was believed that even

this small roughness would significantly increase the heat transfer over a smooth surface. The data show significantly higher heat transfer rates. There are four prediction curves shown in Fig. 7. The curves were obtained using the correlation of Webb et al. (9) times an entrance effect. One pair of curves was calculated using the entrance effect of Ref. 7. The other pair was calculated using the entrance effect from STAN5 results. The entrance effect was calculated as the ratio of the local heat transfer to the fully developed heat transfer rate. This ratio was nearly the same for both the smooth and "rough" calculations, and was not a strong function of the Reynolds number. Comparing Figs. 6 and 7 shows that even small rib heights gave a significant increase in heat transfer over the smooth surface. The higher heat transfer downstream of the entrance and bend is similar to the results for a smooth foil shown in Fig. 6. However, the heat transfer rate decreases more rapidly downstream of the bend, and the STAN5 entrance effect is a better model of the results. The increase in heat transfer from turbulence promoters is most effective when the buffer layer adjacent to the laminar sublayer is fully penetrated by the roughness elements. The height of this layer increases as the Reynolds number is decreased. At the lower Reynolds number the 0.6 percent turbulence promoters may not have completely penetrated this layer.

Figure 8 shows the experimental data and two predictions for tests with 5 percent rib heights. The predictions are the STAN5 entrance effect times Webb's prediction. Again, the local heat transfer in the outlet leg is similar to the heat transfer in the inlet leg. The prediction for each Reynolds number gives higher heat transfer rates than were measured experimentally. The prediction is based on data for tubes with internal ribs. The experimental data are for a ribbed surface with three smooth walls in the passage. Therefore, it is to be expected that the experimental data would have lower heat transfer rates than predicted by the correlation. When the prediction method was compared with the data of Burggraf (4), similar results were found.

With the exception of the smallest size ribs, the turbulence promoters in the present investigation had larger e/D values than were used to correlate the data in Refs. 9 and 10. Reference 9 gives the following equation for the heat transfer ratio for repeated ribs with height e and pitch p when $e^+ > 35$.

$$H_r = \frac{St\ Pr\ Re}{Nu_{fd}}$$

$$= \frac{Pr\ Re\ f/2}{Nu_{fd}\left[1 + \sqrt{\frac{f}{2}}\left(4.5(e^+)^{0.28} Pr^{0.57} - C\left(\frac{p}{e}\right)^{0.53}\right)\right]} \qquad (4)$$

with, $\sqrt{2/f} = 2.5 \ln (D/2e) - 3.75 + C\,(p/e)^{0.53}$

and $e^+ = \frac{e}{D} Re \sqrt{\frac{f}{2}}$

In Ref. 9 the suggested value of C is 0.95, and this value was used for the predictions shown in Figs. 7 to 10. The data in Ref. 10 show that C could range up to 1.2. For the 5 percent ribs the effect of changing C from 0.95 to 1.2 is to decrease the heat transfer by 11 percent. This results in good agreement with the experimental data. The data in Refs. 9 and 10 were for cases where the e/D of square-rib turbulence promoters did not exceed 4 percent. Table I gives the values of C which correlates the experimental data for this investigation. This correlation was applied away from the entrance and bend. Because all tests were done with a p/e of 10, there was no way to determine if the exponent for the pitch ratio term should also be changed for large ribs.

Figure 9 shows experimental data for tests with ribs that were 10 percent of the passage height. These results are similar to the results shown in Fig. 8 for ribs 5 percent of the passage height. Because of the larger rib heights, the disagreement in the asymptotic regions, away from the entrance or bend, between the data and Webb's unmodified prediction is greater. In these tests the thermocouples were at fixed locations relative to the ribs. On the inlet leg they were either at a pitch of 4 relative to the start of the rib, or at a pitch of 9. On the outlet leg, where the flow direction was reversed, the thermocouples were at pitches of 2 and 7. This raised the possibility of a bias in the results if all thermocouples in one of the legs read in a region of low heat transfer. Tests were run with the flow direction reversed. This did not result in a significant change in the results. The data shown in Fig. 9 are for different power levels at the different Reynolds numbers. The foil temperatures were approximately the same for both Reynolds numbers. If foil conduction was significantly affecting the apparent heat transfer, the temperature gradients would be noticeably less at the lower Reynolds number. They were not. The attachment over a 1.5 mm area, (a distance longer than one pitch), may have resulted in an average temperature over a finite area, rather than a point value.

Figure 10 shows the experimental data for tests with 15 percent rib heights. Results are given for Reynolds numbers of 20 000 and 100 000, and two level prediction lines are shown. The predictions are from Webb's unmodified correlation only, and do not included any entrance effect. There is a large amount of scatter in the experimental data. This is the result of some thermocouples reading temperatures in regions where the flow is attached, while others give readings where the flow is not attached. Since no smooth curve would fit the heat transfer data for either leg of the passage, comparisons are made on the basis of the overall relative heat transfer rate. Table II shows a comparison of the overall relative heat transfer rates for different tests. These values were calculated by integrating the local relative heat transfer rates over the entire passage length. Even though the overall heat transfer rates for the 15 percent ribs are less than those predicted from Webb's correlation, they are consistent with the results of Norris (11). The results of this reference indicate that the maximum increase in the overall heat transfer rate for rough surfaces is about 2.6 times the rate for smooth surfaces.

Additional tests were run with ribs 15 percent of the passage height. In these tests the ribs were formed from Bakelite, and were glued to a smooth foil. The purpose of these tests was to determine if a significant portion of the increased heat transfer was due to the fin effect of the integral ribs. Comparisons of the heat transfer rates for the integral ribs and the glued-on Bakelite ribs are given in Fig. 11, and in Table II. If the fin effect of the integral ribs was substantial, the glued-on ribs would result in lower heat transfer. The results show that the glued-on Bakelite ribs had somewhat higher heat transfer rates than the integral ribs. This indicates that the increased heat transfer for ribbed surfaces is the result of the turbulence promoted by the ribs, and not a fin effect. The tests for the glued-on ribs were done with the opposite wall having integral ribs of

the same size. This is in contrast to the other tests with turbulence promoters in which the opposite wall was smooth. This may have resulted in the glued-on ribs having a higher overall heat transfer rate than the integral ribs. Measurements of the heat transfer rates for the integral ribs showed an increase in the heat transfer of about 10 percent compared to that measured when the integral ribbed foil was opposite a smooth foil.

The local heat transfer rates for a smooth surface opposite a rough surface are shown in Fig. 12. Results are shown for a smooth surface opposite 5 and 15 percent ribs. Results are about the same as for a smooth foil opposite a smooth foil as shown in Fig. 6.

Figure 13 shows the change in pressure loss coefficients due to the presence of different size ribs. The data are for the case where one surface had turbulence promoters and the other surfaces were smooth. The data are the difference between the overall loss coefficient and the measured loss coefficient when all surfaces were smooth. The data are at a Reynolds number of 100 000, and similar results were obtained for Reynolds numbers greater than 40 000. Below this value there were large fluctuations in the calculated loss coefficient. The pressure loss results are similar to the heat transfer results in that the smallest size ribs show a large fraction of the increase seen by the largest size ribs. These data are for the overall loss coefficient. The same trend in the data, but with smaller changes in the pressure loss coefficients, were obtained from the pressure drop measurements between a tap at the end of the inlet leg and one near the exit of the outlet leg.

Additional pressure measurements were made with two ribbed foils. One case had foils with 0.6 and 15 percent ribs. In the second test there were two foils with 15 percent ribs. In the first case the loss coefficient was 4.4 greater than the loss coefficient for all smooth walls. This increase contrasts with an increase of 2.5 from Fig. 13 assuming that the increase for two ribbed surfaces is the sum of the increase for each surface. The increase for two foils with 15 percent ribs was 10.5. This compares with an increase of 2.8 assuming that the increase for two ribbed surfaces was additive. This showed that large ribs on both walls compound the pressure drop in the passage.

CONCLUSIONS

The tests with smooth walls showed that the bend geometries tested did not significantly affect the heat transfer or pressure drop. The local heat transfer was about the same for the rectangular bend, the semi-circular bend, or the one with rounded corners. For all three bends the heat transfer increased with position through the bend. Downstream of the bend the heat transfer rates indicated that the boundary layer reformed in the same manner as it did after the 90° inlet bend. To predict the local heat transfer along the passage it is necessary to use the empirical correlation given in Ref. 7 for the data of Ref. 5.

Away from the entrance or bend regions the heat transfer for surfaces with turbulence promoters can be predicted by the correlation of Webb et al., when limited according to the results of Norris. For turbulence promoters of moderate size the heat transfer rate along the passage could be predicted as a multiplier of the entrance effect from STAN5 by the bounded correlation of Webb et al.. For the ribs with a height-to-diameter ratio of 15 percent the entrance effect was not strongly evident.

The results indicate that the heat transfer reaches a maximum with rib heights of about 5 percent. The pressure loss increased slowly with rib height when there is only one ribbed surface. Therefore, rib heights of about 5 percent would make the most effective use of blade cooling air. The optimum rib height would be somewhat less if ribs were used on more than one wall. This result is based on results for only a single pitch-to-height ratio, other ratios might result in a somewhat different optimum configuration.

REFERENCES

1. Graham, R. W., "Fundamental Mechanisms That Influence the Estimate of Heat Transfer to Gas Turbine Blades," ASME Paper No. 79-HT-43, Aug. 1979.
2. Holland, M. J., and Thake, T. F., "Rotor Blade Cooling In High Pressure Turbines," Journal of Aircraft, Vol. 17, No. 6, June 1980, pp. 412-418.
3. Bergles, A. E., and Webb, R. L., "Bibliography on Augmentation of Convective Heat and Mass Transfer," Augmentation of Convective Heat and Mass Transfer," E. Bergles and R. L. Webb, eds., ASME, 1970, pp. 1-15.
4. Burggraf, F., "Experimental Heat Transfer and Pressure Drop with Two-Dimensional Discrete Turbulence Promoters Applied to Two Opposite Walls of a Square Tube," Augmentation of Convective Heat and Mass Transfer," E. Bergles and R. L. Webb, eds., ASME, 1970, pp. 70-79.
5. Boelter, L. M. K., Young, G., and Iversen, H. W., "An Investigation of Aircraft Heaters. XXVII - Distribution of Heat-Transfer Rate in the Entrance Section of a Circular Tube," NACA TN-1451, 1948.
6. McAdams, W. H., Heat Transmission, 3rd ed., McGraw-Hill, New York, 1954.
7. Kays, W. M., Crawford, M. E., "Convective Heat and Mass Transfer," 2nd ed., McGraw-Hill, New York, 1980.
8. Crawford, M. E., Kays, W. M., "STAN5: A Program for Numerical Computation of Two-Dimensional Internal and External Boundary Layer Flows," NASA CR-2742, 1976.
9. Webb, R. L., Eckert, E. R. G., and Goldstein, R. J., "Heat Transfer and Friction in Tubes with Repeated-Rib Roughness," International Journal Heat and Mass Transfer, Vol. 14, Apr. 1971, pp. 601-617.
10. Webb, R. L., Eckert, E. R. G., and Goldstein, R. J., "Generalized Heat Transfer and Friction Correlations for Tubes with Repeated-Rib Roughness," International Journal Heat and Mass Transfer," Vol. 15, Jan. 1972, pp. 180-184.
11. Norris, R. H., "Some Simple Approximate Heat-Transfer Correlations for Turbulent Flow in Ducts with Rough Surfaces," Augmentation of Convective Heat and Mass Transfer," E. Bergles and R. L. Webb, eds. ASME, 1970, pp. 16-26.

TABLE I. - COMPARISON OF THE RELATIVE OVERALL RELATIVE HEAT TRANSFER RATE

Reynolds number	Overall relative heat transfer rate, $\overline{H}_r$					
	Type of surface heated					
	Smooth	0.6 percent ribs	5 percent ribs	10 percent ribs	15 percent ribs (intergal)	15 percent ribs (glued-on)
20 000	1.75	2.32	2.92	2.58	2.46	2.85
100 000	1.60	2.60	2.55	2.31	2.24	2.45

TABLE II. - COEFFICIENTS TO MATCH EXPERIMENTAL HEAT TRANSFER RATIO AWAY FROM ENTRANCE OR BEND

Reynolds number	Rib height, e/D, percent									
	0.6 percent		5 percent		10 percent		15 percent		[a]15 percent	
	$H_{r,\infty}$	C	$H_{r,\infty}$	C	$H_{r,\infty}$	C	$H_{r,\infty}$	C	$H_{r,\infty}$	C
20 000	1.4	[b]	2.3	1.3	2.2	1.7	2.2	1.9	2.3	1.8
100 000	1.6	1.3	2.0	1.5	2.0	1.7	2.0	1.8	2.0	1.8

[a] Glued-on Bakelite ribs.
[b] $e^+ < 35$.

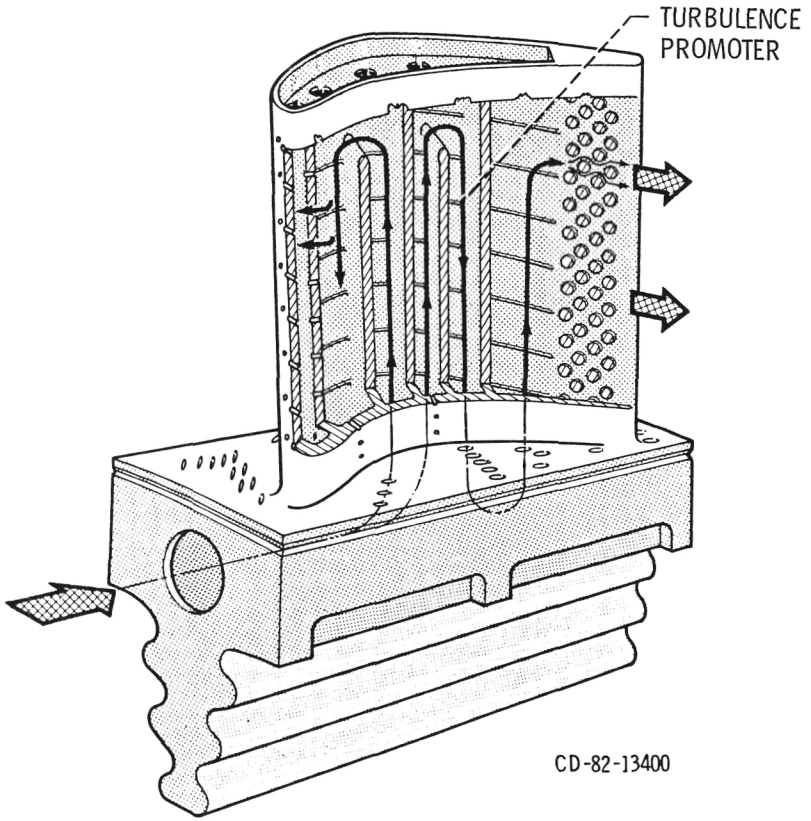

Figure 1. - Turbine blade with serpentine cooling passages.

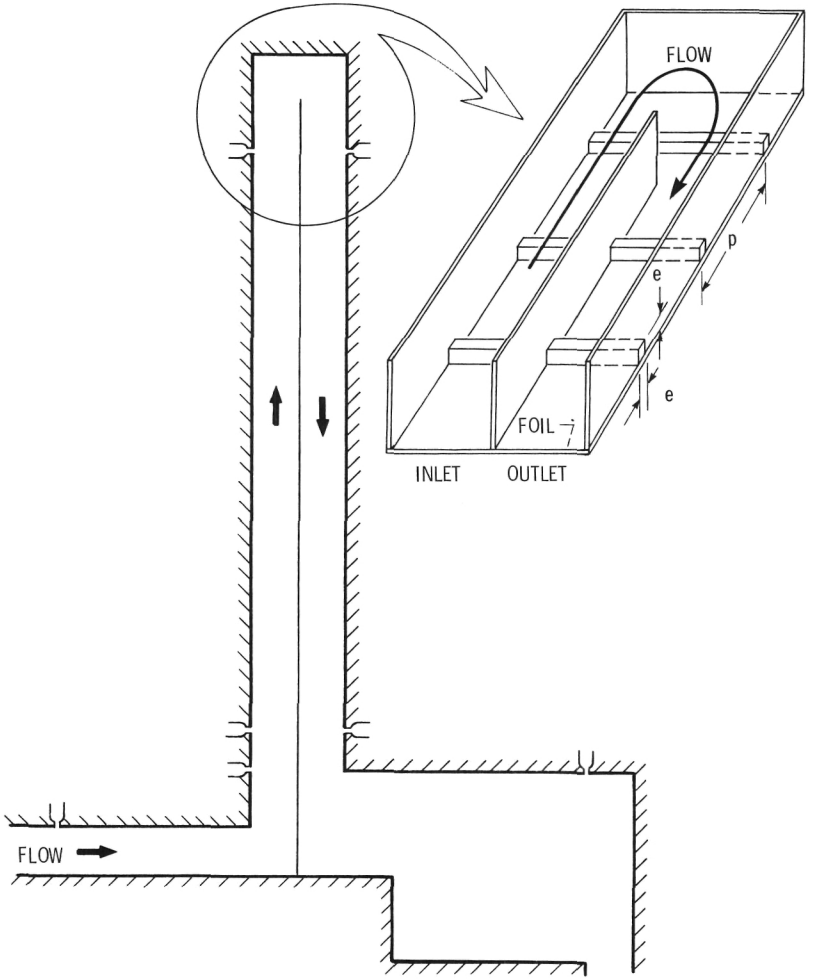

Figure 2. - Schematic for test section.

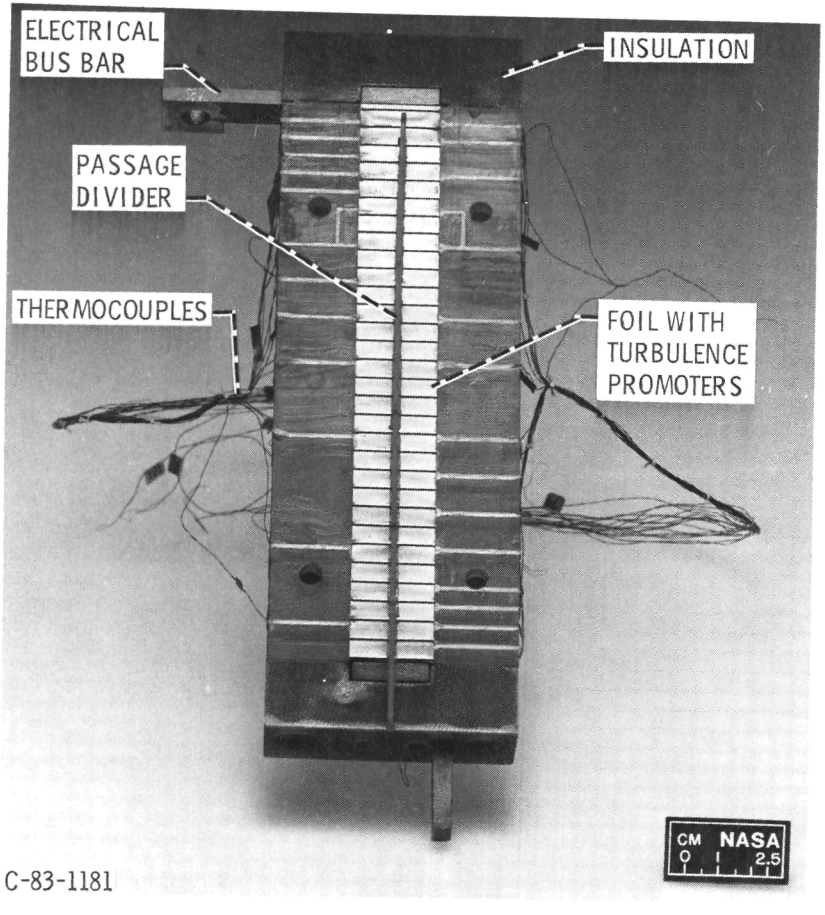

Figure 3. - Upper foil test section.

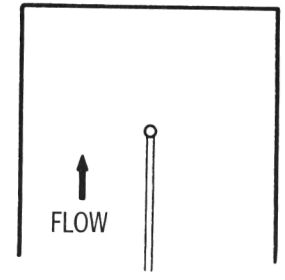

(a) Rectangular.

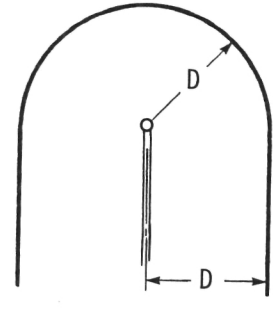

(b) Semi-circular.

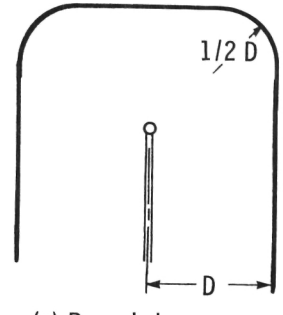

(c) Rounded corners.

Figure 4. - Schematic of different bend geometries.

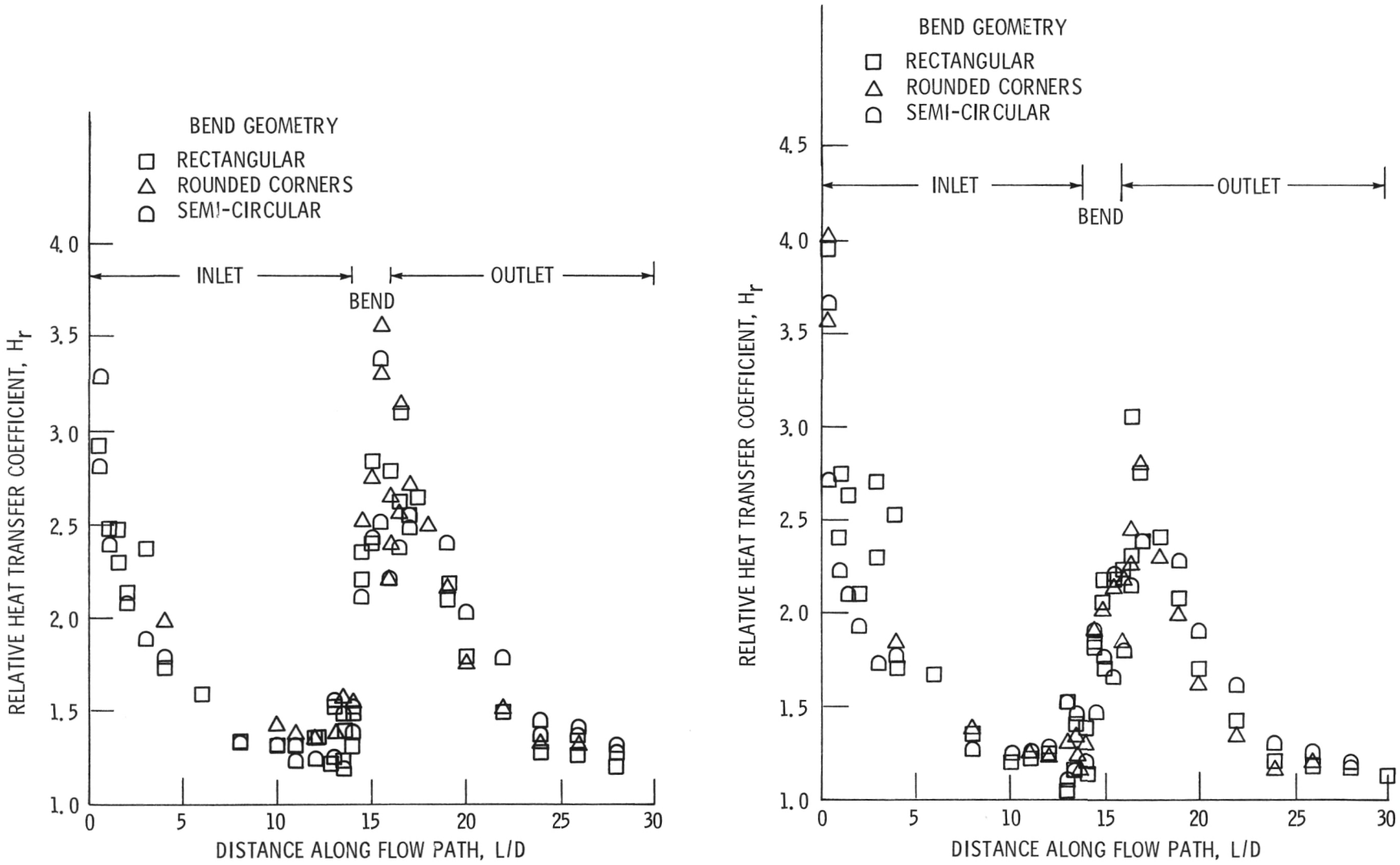

(b) Reynolds number, 60 000.

Figure 5. - Continued.

(c) Reynolds number, 20 000.

Figure 5. - Comparison of measured heat transfer rates for different bend geometries and smooth walls.

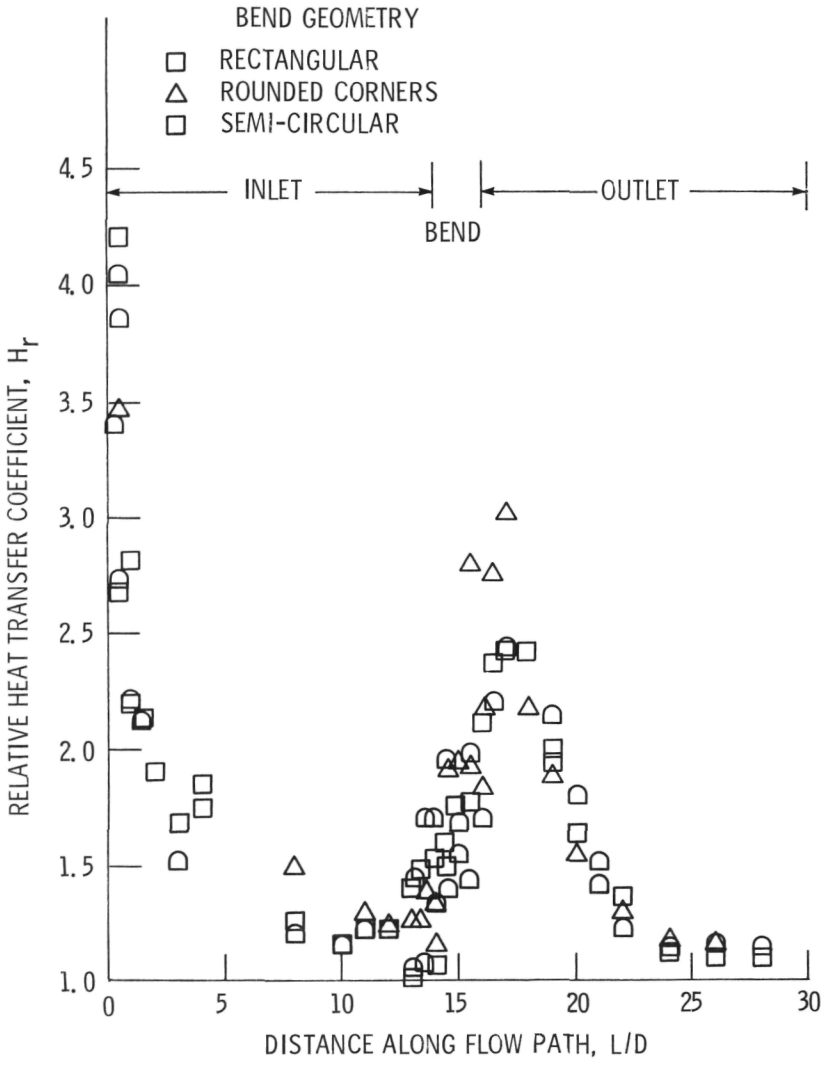

(c) Reynolds number, 100 000.

Figure 5. - Concluded.

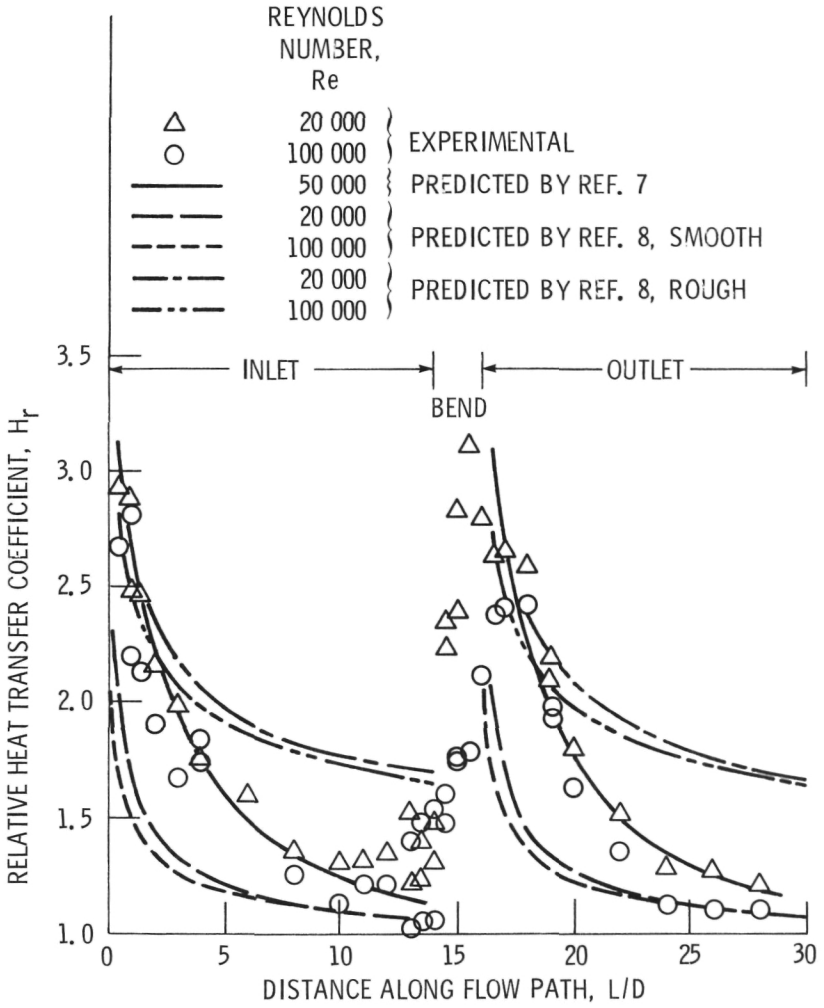

Figure 6. - Measured and predicted heat transfer rates for rectangular bend geometry.

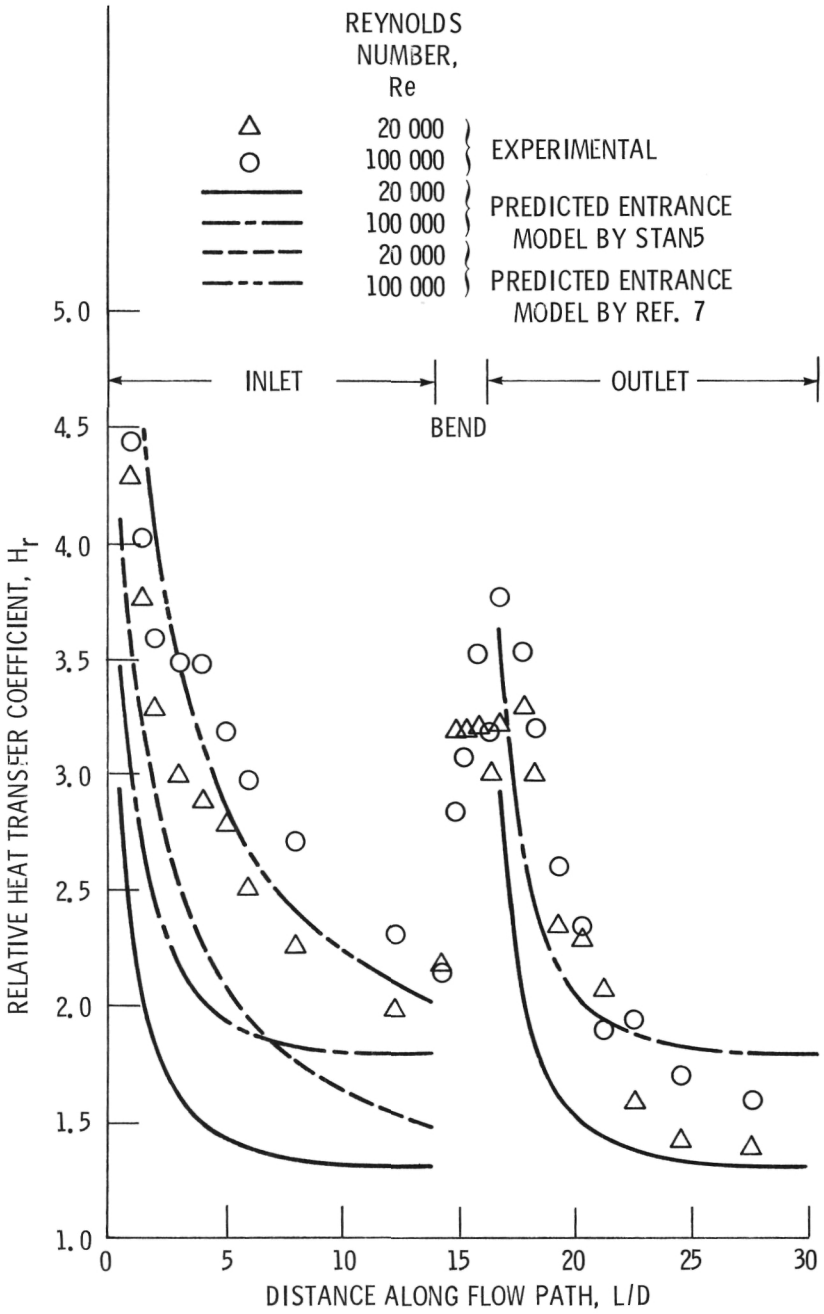

Figure 7. - Measured and predicted heat transfer rates for 0.6 percent rib heights.

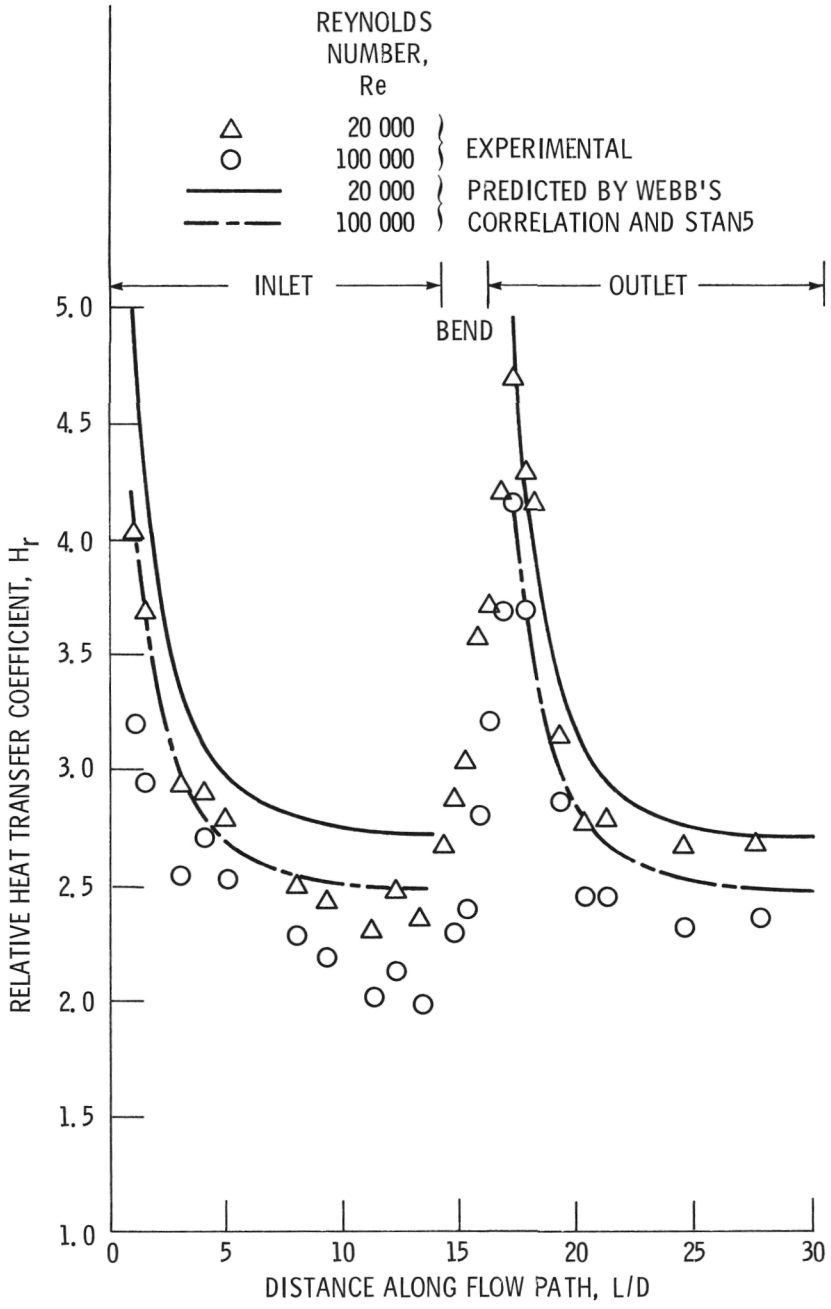

Figure 8. - Measured and predicted heat transfer rates for 5 percent rib heights.

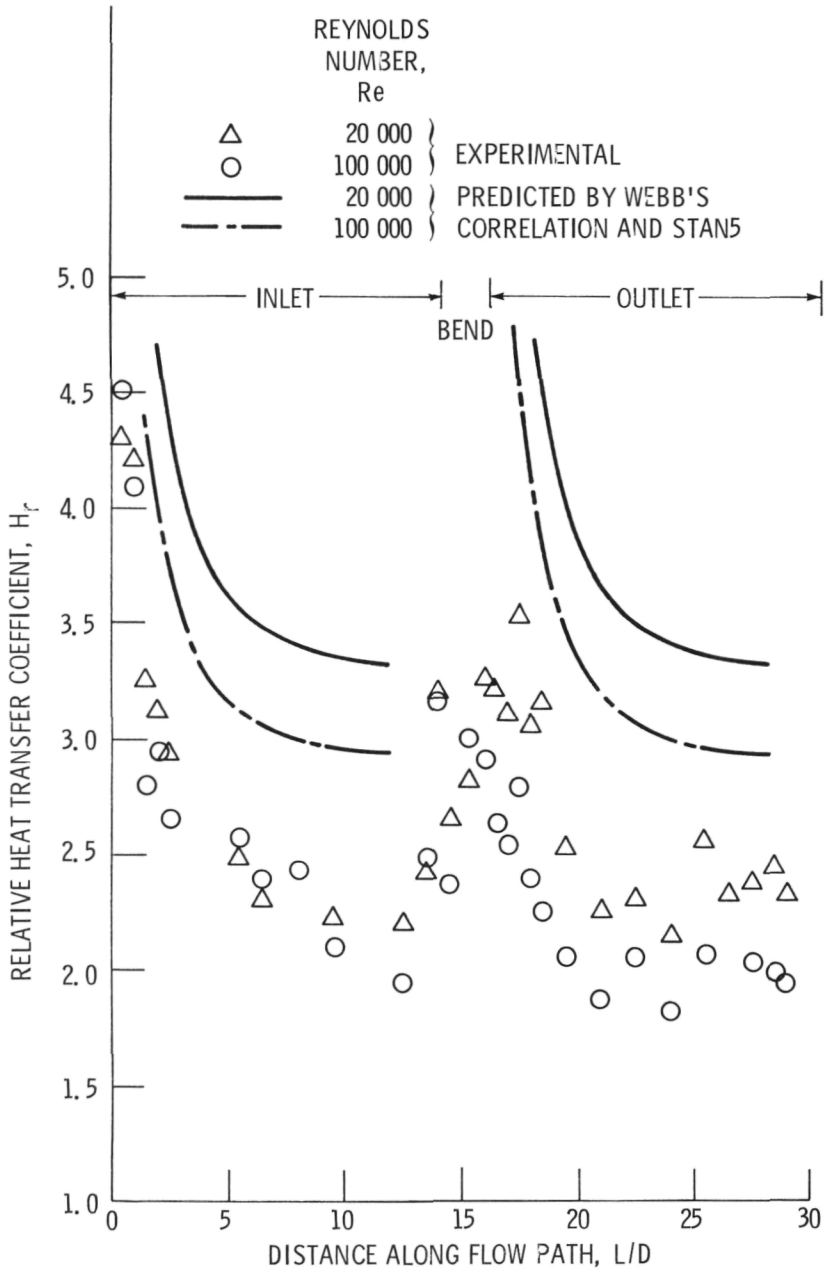

Figure 9. - Measured and predicted heat transfer rates for 10 percent rib heights.

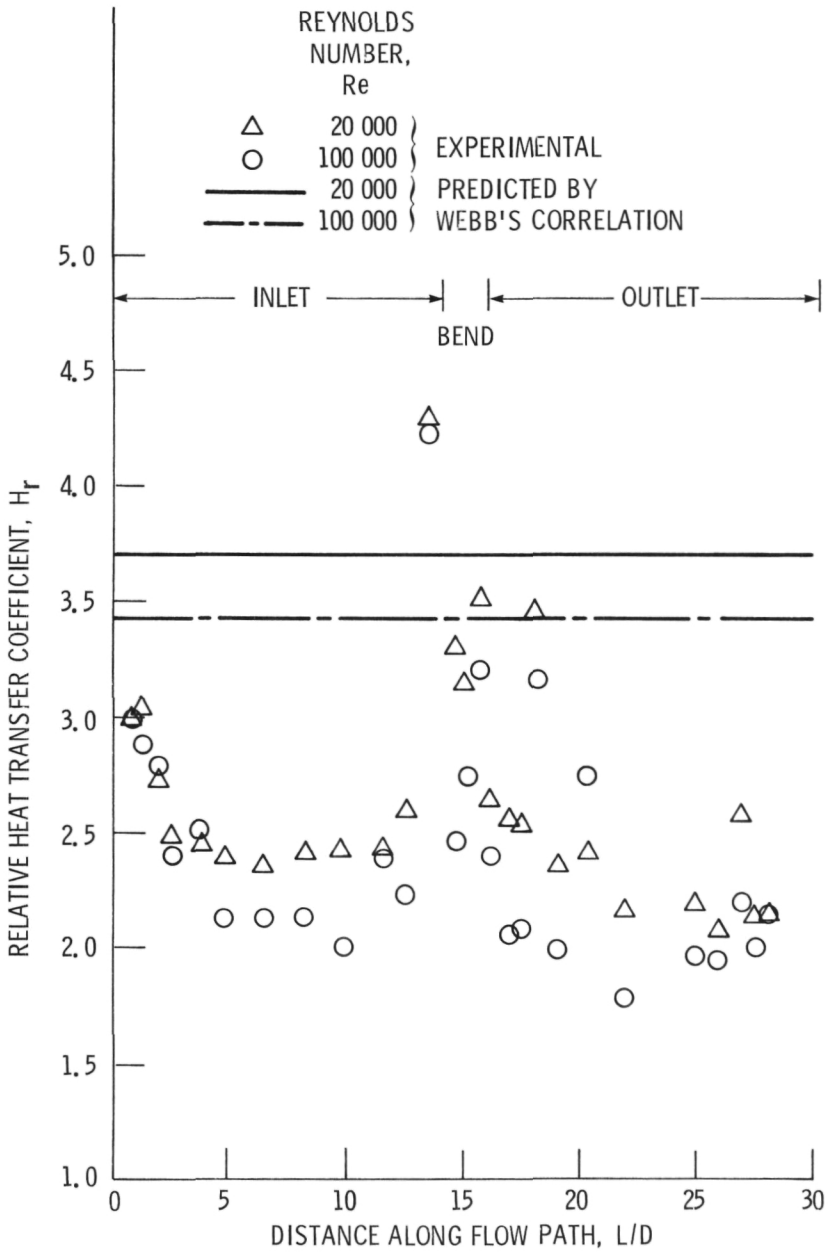

Figure 10. - Measured and predicted heat transfer rates for 15 percent rib heights.

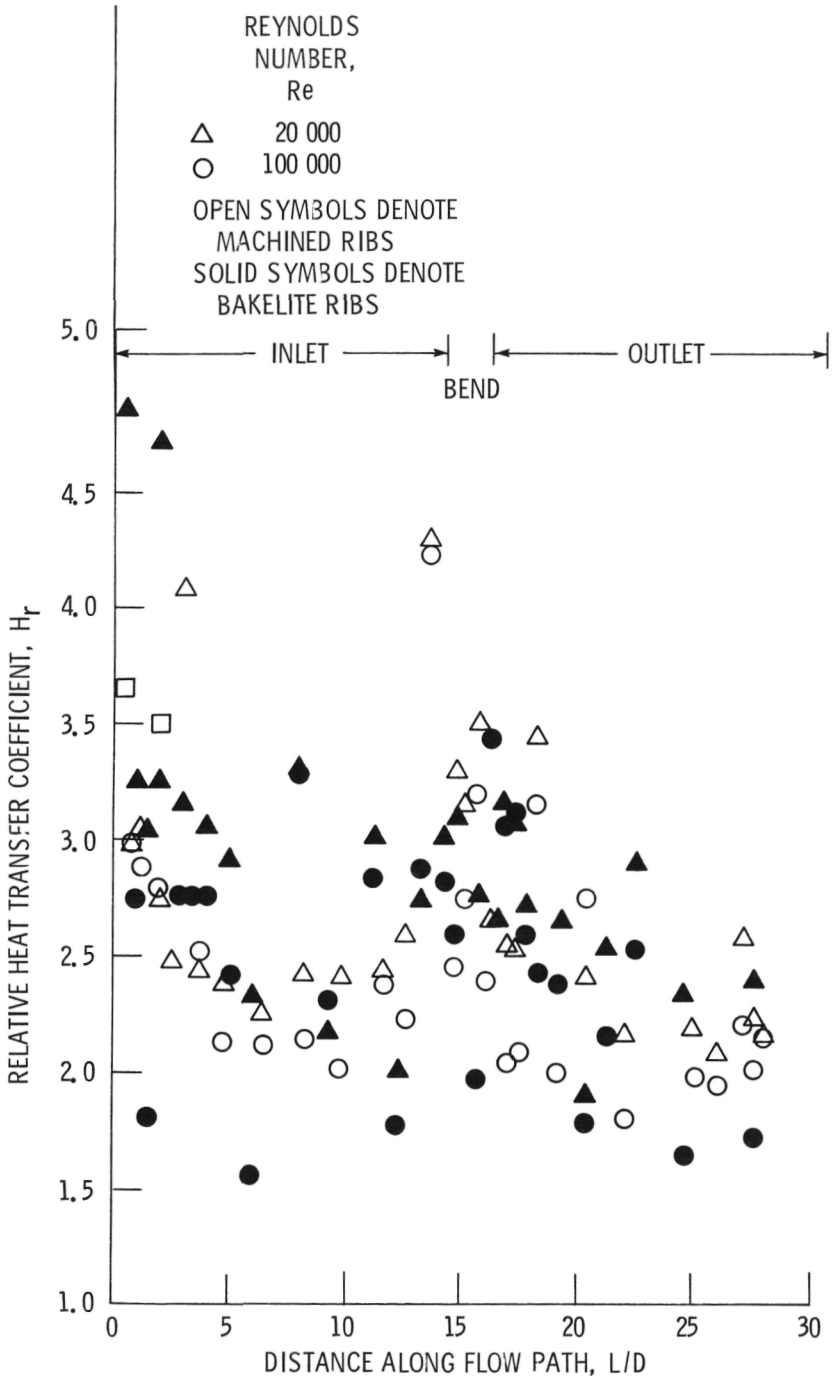

Figure 11. - Heat transfer rate for machined ribs and ribs glued to smooth foil. Rib height, 15 percent.

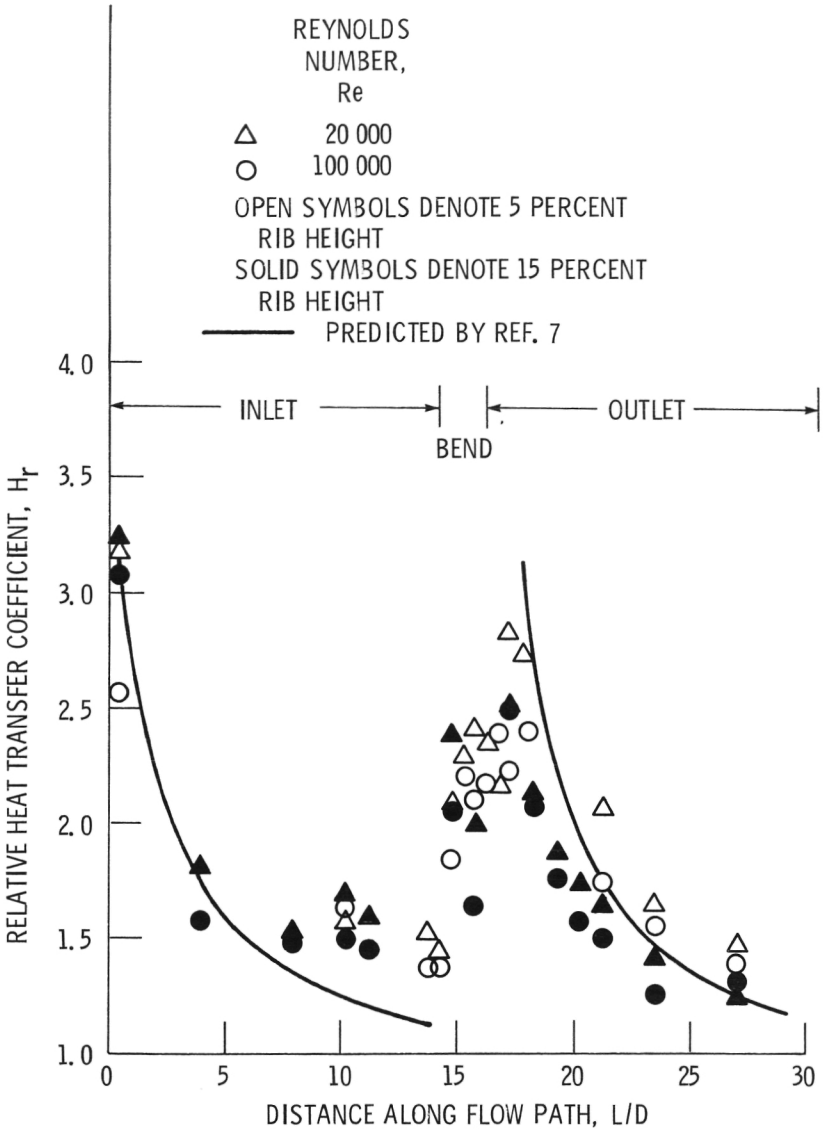

Figure 12. - Heat transfer rate for a smooth surface opposite a ribbed surface.

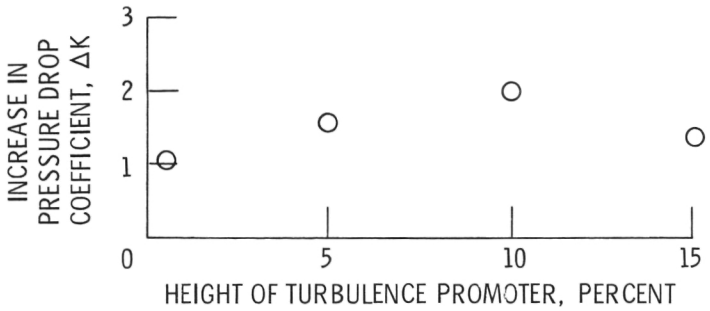

Figure 13. - Increase in pressure drop coefficient due to having turbulence promoters on one surface.

1. Report No.	2. Government Accession No.	3. Recipient's Catalog No.
NASA TM-83614		

4. Title and Subtitle	5. Report Date
Heat Transfer in Serpentine Passages With Turbulence Promoters	6. Performing Organization Code 505-31-42

7. Author(s)	8. Performing Organization Report No.
Robert J. Boyle	E-2040
	10. Work Unit No.

9. Performing Organization Name and Address	11. Contract or Grant No.
National Aeronautics and Space Administration Lewis Research Center Cleveland, Ohio 44135	13. Type of Report and Period Covered Technical Memorandum

12. Sponsoring Agency Name and Address	14. Sponsoring Agency Code
National Aeronautics and Space Administration Washington, D.C. 20545	

15. Supplementary Notes

Prepared for the Twenty-second National Heat Transfer Conference cosponsored by the ASME and AIChE, Niagara Falls, New York, August 5-8, 1984.

16. Abstract

Local heat transfer rates and overall pressure losses were determined for serpentine passages of square cross section. The flow entered an inlet leg, turned 180° and then passed through an outlet leg. Two series of tests were done. First, results were obtained for a passage with smooth walls for three different bend geometries. Second, the effect of turbulence promoters was investigated. Tests were done for turbulence promoters between 0.6 and 15 percent of the passage height. Gaseous nitrogen was the working fluid, and the Reynolds number varied between 20 000 and 100 000. Local heat transfer rates were determined from thermocouple measurements on a thin electrically heated Inconel foil. Pressure drop measurements were made along the flow path.

17. Key Words (Suggested by Author(s))	18. Distribution Statement
Turbine blade; Cooling; Augmentation; Turbulent heat transfer	Unclassified - unlimited STAR Category 34

19. Security Classif. (of this report)	20. Security Classif. (of this page)	21. No. of pages	22. Price*
Unclassified	Unclassified		

*For sale by the National Technical Information Service, Springfield, Virginia 22161